

## Expression, Purification and Characterization of Critical Domains of Munc13-1

Cong MA<sup>1</sup>, Hai HOU<sup>2</sup>, Wei TIAN<sup>1</sup>, and Tao XU<sup>1,2\*</sup>

<sup>1</sup> Joint Laboratory of Huazhong University of Science and Technology and Institute of Biophysics, College of Life Science and Technology, Huazhong University of Science and Technology, Wuhan 430074, China;

<sup>2</sup> National Laboratory of Biomacromolecules, Institute of Biophysics, Chinese Academy of Sciences, Beijing 100101, China

**Abstract** Munc13-1 is an essential component of synaptic vesicle releasing machinery. Three rat Munc13-1 constructs were rationally designed based on homology and function, overexpressed in *Escherichia coli*, and purified to homogeneity with a final yield higher than 2 µg/ml of cell culture. The purified Munc13-1 recombinant proteins had distinct oligomeric states, monodispersity and homogeneity properties. Their secondary structural contents were analyzed by the circular dichroism method, and the sedimentation coefficients of these recombinant proteins were measured by analytical ultracentrifugation. The long helical bundle-like topology of Munc13-1 was first revealed by analysis of our data. In addition, these purified recombinant proteins provide ideal starting materials for further biochemical, biophysical, and structural studies on mammalian Munc13 proteins.

**Keywords** Munc13-1; monodispersity; circular dichroism; analytical ultracentrifugation; sedimentation coefficients

Synaptic vesicles are the key organelles in neurotransmitter release at synapses. A crucial step in synaptic vesicle exocytosis is priming, which confers fusion competence to docked vesicles, enabling them to undergo rapid exocytosis upon sensing Ca<sup>2+</sup> influx [1]. Recent evidence indicates that synaptic vesicle priming requires proteins of the Munc13/UNC-13 family. UNC-13 was originally identified in *Caenorhabditis elegans* [2], and Munc13 proteins, as mammalian UNC-13 homologs, constitute a family of four members, namely Munc13-1, -2, -3, and -4. These Munc13 isoforms are differentially expressed in brain, except Munc13-4 which predominantly expresses in non-neuronal tissues [3–7].

Munc13-1 is a multi-domain protein consisting of 1735 amino acid residues. It contains a phorbol ester binding C1 domain and three C2 domains [8,9]. Genetic deletion of *Munc13-1/unc13* genes causes total arrest of synaptic transmission due to a complete loss of fusion-competent

synaptic vesicles [3,10–13]. Some evidence has suggested that, in the carboxyl (C)-terminal half of Munc13-1, the region of residues 1181–1345 interacts with the amino (N)-terminal coiled-coil domain of syntaxin 1A, and this interaction appears to be compatible with soluble N-ethylmaleimide-sensitive attachment protein receptor (SNARE) complex assembly [14]. However, this interaction has not been further characterized or verified with more evidence. Moreover, initially identified in distantly related Munc13-like proteins from *Saccharomyces cerevisiae* and *Schizosaccharomyces pombe* [7], Munc13 homology domain (MHD) has been found to be present in a wide variety of species from *Arabidopsis thaliana*, *C. elegans* and *Drosophila melanogaster*, to mouse, rat and human.

The crucial role of Munc13-1 during vesicle priming has been shown to be associated with its 859–1531 fragment, which is sufficient to rescue impaired vesicle releasing in Munc13-1/2 double knockout mice [15]. In addition, using Munc13-1 deletion constructs in an electrophysiological gain-of-function assay of chromaffin-granule secretion, it is shown that the priming activity can be mediated by the Munc13-1 C-terminal region of residues 1100–1735 (**Fig. 1**) [16].

DOI: 10.1111/j.1745-7270.2007.00316.x

Received: March 18, 2007 Accepted: April 30, 2007

This work was supported by the grants from the National Natural Science Foundation of China (30470448, 30130230), and the Major State Basic Research Program of China (2004CB720000)

\*Corresponding author: Tel, 86-10-64888469; Fax, 86-10-64867566; E-mail, xutao@ibp.ac.cn

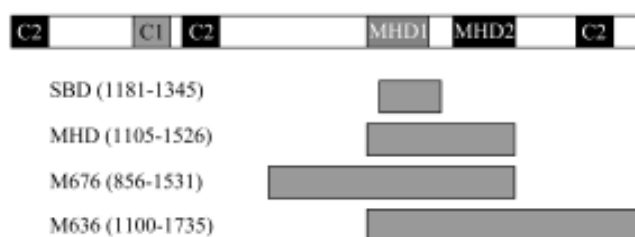


**Fig. 1 Schematic domain structure of Munc13-1 and representation of constructs**

The domain boundaries of Munc13-1 were selected based on Koch *et al.* [7]. M636, minimal activity domain II; M676, minimal activity domain I; MHD, Munc13 homology domain; SBD, syntaxin binding domain.

To date, 3-D structures of the C1 domain and the N-terminal C2 domain of Munc13-1 have been reported [17, 18]. The 3-D structures of the full-length Munc13 proteins, their MHD domains, or other above-mentioned functional fragments, however, have not been reported. One difficulty towards structural study of these proteins appears to be obtaining a large quantity of purified recombinant Munc13 proteins.

In this paper, we report the overexpression and purification of recombination proteins of several rat Munc13-1 constructs and characterization of their oligomeric states, monodispersity and protein stability.

## Materials and Methods

### Cloning of Munc13-1 constructs

Munc13-1 constructs were designed based on sequence homology analysis and results from previous functional studies [7,14–16]. cDNAs were amplified from the full-length rat *Munc13-1* gene (GenBank accession No. U24070) by polymerase chain reaction. All constructs contained a 5'-end *Bam*HI restriction site and a 3'-end *Eco*RI restriction site. The amplified Munc13-1 constructs were then digested by *Bam*HI and *Eco*RI restriction enzymes and ligated into both the pET28a vector (Novagen, Darmstadt, Germany) encoding for thrombin cleavable N-terminal His<sub>6</sub>-tagged fusion proteins and the pGEX6p-1 vector (Amersham-Pharmacia Biotech, Piscataway, USA) encoding for PreScission protease (Amersham-Pharmacia Biotech) cleavable N-terminal glutathione S-transferase (GST)-tagged fusion proteins. The ligated plasmids were transformed into *Escherichia coli* DH5 $\alpha$  for amplification. All cloned Munc13-1 constructs were confirmed by DNA

sequencing and subsequently transformed into *E. coli* BL21 (DE3) for protein expression.

### Expression and purification of Munc13-1 constructs

All recombinant proteins were expressed in *E. coli* BL21 (DE3) cells according to standard protocols. Briefly, a 4-L Luria-Bertani culture was inoculated with overnight culture and grown for 3 h, starting at 37 °C. Thirty minutes prior to induction, the culture temperature was gradually lowered to 16 °C, followed by induction at  $A_{600}$  of 1.0 with 0.5 mM isopropyl- $\beta$ -D-thiogalactopyranoside. Cells were harvested 20 h after induction at  $A_{600}$  of 8.0.

All purification steps were carried out at 4 °C. For His<sub>6</sub>-tagged fusion proteins, total cell paste was harvested and suspended in lysis buffer [50 mM Tris-HCl (pH 8.0), 500 mM NaCl, 10% (*V/V*) glycerol, 20 mM imidazole and 1 mM dithiothreitol (DTT)]. After repeated rounds of sonication, the lysate was centrifuged at 12,000 *g* for 30 min. The supernatant was loaded on a 5 ml column of Ni<sup>2+</sup>-NTA agarose (Qiagen, Hamberg, Germany) pre-equilibrated and washed with the lysis buffer. The target proteins were obtained with elution buffer [50 mM Tris-HCl (pH 8.0), 500 mM NaCl, 10% (*V/V*) glycerol, 500 mM imidazole, and 1 mM DTT]. The His tag was removed by incubation with thrombin (10 U/mg protein; Sigma-Aldrich, St. Louis, USA) overnight at 4 °C. For GST-tagged proteins, the supernatant was mixed with 5 ml of glutathione-Sepharose (Amersham-Pharmacia Biotech) after sonication and centrifugation. Phosphate-buffered saline was used to pre-equilibrate the column and to wash off non-specific binding. GST fused PreScission protease (10 U/mg protein) was added to the column and incubated overnight at 4 °C to remove the GST tag from the target protein.

After the salt concentration was lowered to 20 mM by dilution, the tag-removed sample was further purified by ion-exchange chromatography. In general, the sample was loaded onto a 5 ml Q-Sepharose FastFlow column (Amersham-Pharmacia Biotech) pre-equilibrated with loading buffer [20 mM Tris-HCl (pH 8.5) and 20 mM NaCl]. Following washing with 10 ml loading buffer, the column was eluted with a 60 ml 0–1.0 M linear NaCl gradient at a rate of 1.0 ml/min. The purity of all protein samples was verified by Coomassie Blue stained 12% sodium dodecyl sulfate-polyacrylamide gel electrophoresis (SDS-PAGE).

### Determination of oligomeric state and monodispersity by size exclusion chromatography (SEC)

Each recombinant protein sample was concentrated to

10 mg/ml using a YM10 centricron (Amicon, Beverly, USA) and applied to a preparative size exclusion Superdex G-200 column on a fast protein liquid chromatography instrument (Amersham-Pharmacia Biotech) in the presence of 20 mM Tris-HCl (pH 8.0), 150 mM NaCl and 1 mM DTT. Concentration of the eluted protein was measured using a bicinchoninic acid assay (Pierce, Rockford, USA).

### Determination of sedimentation coefficient by analytical ultracentrifugation

Sedimentation experiments were carried out using an XL-I analytical ultracentrifuge (Beckman Coulter, Fullerton, USA) equipped with a four-cell An-60 Ti rotor at 20 °C. Sedimentation velocity experiments were carried out at a speed of 40,000–60,000 rpm for Munc13-1 constructs at a concentration of 0.5–1.0 mg/ml. Scans were taken at 280 nm wavelength with a radial step size of 30  $\mu$ m. Differential sedimentation coefficients,  $c(s)$ , were calculated by least square boundary modeling of the sedimentation velocity data using the software program SEDFIT (National Institutes of Health, Bethesda, USA)[19]. The values of apparent sedimentation coefficients were converted to  $S_{20,w}$  for solvent viscosity using the program SEDNTERP ([www.jphilo.mailway.com/download.htm](http://www.jphilo.mailway.com/download.htm)). The frictional coefficients ( $f/f_0$ ) and axial ratios ( $a/b$ ) were calculated using the  $V_{bar}$  method in SEDNTERP.

### Circular dichroism (CD) spectrometry

Far ultraviolet (190–260 nm) CD spectra were measured with a Jasco J-715 spectrometer. The protein concentration was 0.3 mg/ml, buffered with 20 mM Tris-HCl (pH 8.0), 150 mM NaCl and 1 mM DTT. The wavelength scan was carried out at 0.5 nm intervals in a 0.1 cm quartz cuvette at 20 °C. Spectra were digitized by recording in milli-degree increments, and these values were then converted to per residue molar absorption (in mdeg/M/cm units). Experimental CD spectra were used to estimate the composition of secondary structures of the target protein using the K2D program at the DICROWEB website (<http://www.cryst.bbk.ac.uk/cdweb/html/home.html>) [20,21].

## Results

### Rational design of Munc13-1 constructs

Previously, it was reported in a GST-mediated pull down assay that a fragment (residues 1181–1345) of rat Munc13-1 binds syntaxin 1A [14] and this interaction needed to be further confirmed. Subsequently, sequence analysis of

distantly related Munc13-like proteins indicated that there are two conserved Munc13 homology domains, named MHD1 (residues 1106–1249) and MHD2 (residues 1358–1525) in rat Munc13-1 [7]. To date, two similar minimal activity domains have been defined independently by two research groups [15,16], one of which spans 676 amino acids (residues 859–1531), and the other spans 636 amino acids (residues 1100–1735). Based on available information, therefore, we designed and examined four distinctive but overlapped Munc13-1 constructs, termed the syntaxin binding domain (SBD, residues 1181–1345), minimal activity domain I (M676, residues 856–1531), minimal activity domain II (M636, residues 1100–1735), and MHD (MHD1 and MHD2, residues 1105–1526) (Fig. 1).

### Expression of Munc13-1 recombinant proteins in *E. coli*

To optimize the solubility and yield of the recombinant proteins, two expression vectors, pET28a and pGEX6p-1, were used in our study resulting in fusion proteins of either a N-terminal His<sub>6</sub>-tag or a N-terminal GST-tag. Thus, the four aforementioned Munc13-1 constructs were combined with these two vectors resulting in six recombinant proteins, namely His-tagged SBD and MHD and GST-tagged SBD, MHD, M676, and M636. All of them were expressed in *E. coli* BL21 with LB culture. Moreover, lowering the cell culture temperature from 37 °C to 16 °C prior to isopropyl- $\beta$ -D-thiogalactopyranoside (IPTG) induction effectively prevented formation of inclusion bodies. As shown in Fig. 2(A), all recombinant proteins were expressed at a level higher than 2  $\mu$ g/ml of cell culture, as detected by SDS-PAGE.

### Purification of Munc13-1 recombinant proteins

After glutathione (GSH) affinity purification and PreScission protease digestion to remove the GST tag, the recombinant protein of SBD was obtained at approximately 90% purity [Fig. 2(B)] and stayed soluble at a concentration of 10–20 mg/ml. In contrast, the purified His-tagged SBD was found to precipitate above 3 mg/ml during concentration. Therefore, we focused on the SBD sample initially produced with the GST-tag and used anion exchange chromatography with Q-Sepharose to further purify SBD, which has a PI value of 5.6. Most of the SBD recombinant protein bound to the Q-Sepharose was eluted at a NaCl concentration of 300–400 mM, followed by uncharacterized DNA species at a higher salt concentration (data not shown). Of note, the SBD sample was unstable against thrombin or trypsin digestion.

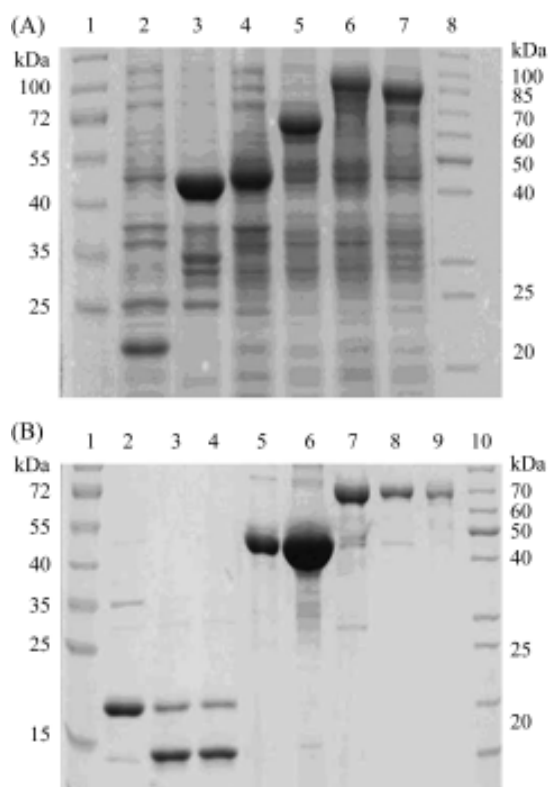


**Fig. 2 Sodium dodecyl sulfate-polyacrylamide gel electrophoresis (SDS-PAGE) of Munc13-1 constructs with or without fusion tags**

SDS-PAGE showing the overexpression and purification of the Munc13-1 constructs with or without fusion tags. (A) SDS-PAGE of whole cell lysates of the Munc13-1 constructs. Lanes 1 and 8, protein markers; lane 2, pET28a-syntaxin binding domain (SBD); lane 3, pGEX6p-SBD; lane 4, pET28a- Munc13 homology domain (MHD); lane 5, pGEX6p-MHD; lane 6, pGEX6p-M676; lane 7, pGEX6p-M636. (B) Purification of the Munc13-1 constructs. Lanes 1 and 10, protein markers; lanes 2–4, SBD after affinity column, Q-Sepharose column and size exclusion chromatography (SEC); lanes 5 and 6, MHD after affinity column and SEC; lanes 7–9, M676 after affinity column, Q-Sepharose column and SEC.

Compared to GST-tagged MHD, His-tagged MHD showed better purity at approximately 95% after elution from the affinity column [Fig. 2(B)]. Thus, the His-tagged recombinant MHD protein was further purified with SEC after removal of the His tag. We found that the purified, tag-less MHD was stable against thrombin or trypsin digestion.

Both M676 and M636 were retained on the GSH column once the GST tag was removed. Whereas M636 could not be recovered from the column, M676 could be desorbed from the column with 0.1% Triton X-100. Redundant Triton X-100 was removed from the solubilized sample by Q-Sepharose column at low salt concentration. The M676 recombinant protein could be eluted with 95% purity

from the Q-Sepharose column at a NaCl concentration of 400–600 mM [Fig. 3(C)]. The PI value of M676 is 5.9. Like MHD, the purified M676 sample was stable against thrombin or trypsin digestion.

### Oligomeric states and monodispersity of purified recombinant proteins of SBD, MHD and M676

The oligomeric states of SBD, MHD and M676 without tags were analyzed by size exclusion fast protein liquid chromatography. SBD was eluted in three peaks. As shown in Fig. 3(A), its oligomeric states ranged from highly polymerized states to a monomeric form on a Superdex G-200 column, determined by the retention time extrapolated from soluble protein standards. The monomer form increased in the presence of 1 mM DTT, suggesting that intermolecular disulfide linkage is a major factor determining the aggregation of SBD. In addition, we found that the SBD sample was unstable at 4 °C and degraded in approximately 24 h from 18 kDa to approximately 15 kDa on SDS-PAGE [Fig. 2(B)].

Analysis of the elution of MHD from the Superdex G-200 column showed that MHD had two sharp peaks. One peak was highly polymerized (peak 1), and the other (peak 2) had a symmetrical shape and an estimated dimer molecular weight [Fig. 3(B)]. Next, we investigated the stability of MHD. After size exclusion purification, the dimeric MHD fraction remained monodispersed in the presence of 1 mM DTT for less than 3 d at 4 °C. Furthermore, most of the dimeric form of the MHD sample would aggregate to the highly polymerized state within 1 d if the two forms remained mixed.

After removing excess detergent, M676 had a single peak with symmetrical shape on the Superdex G-200 column [Fig. 3(D)], which corresponded to the monomeric form. Purified M676 was stable at the monomeric form for more than 1 week at 4 °C.

### Determination of sedimentation coefficient by analytical ultracentrifugation

It is well evident that monodispersity and stability of a protein sample are critical for its crystallization [22]. Monodispersity of our MHD and M676 samples was further verified by analytical ultracentrifugation. The SBD sample was excluded from this investigation because of its instability.

Sedimentation velocity of purified MHD [peak 2 in Fig. 3(B)] showed a single sedimenting boundary at 96.32 kDa with an apparent sedimentation coefficient of 3.98 S [Table 1 and Fig. 4(A)]. Considering the calculated molecular weight of 47.91 kDa for MHD, the data indicated

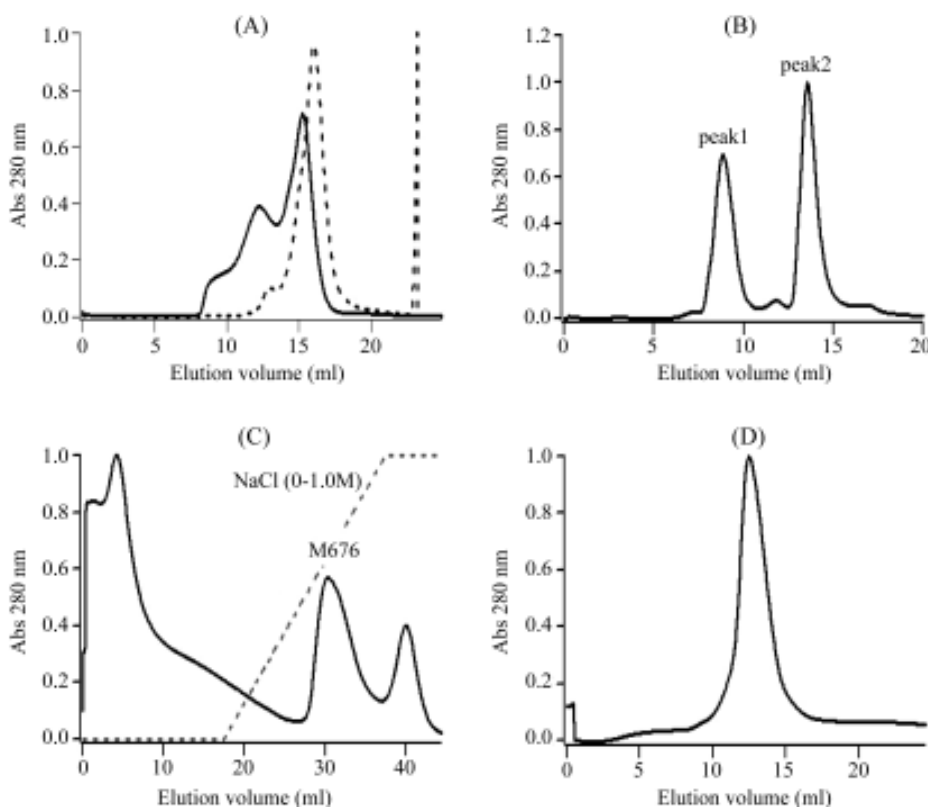


**Fig. 3 Oligomeric state and monodispersity of Munc13-1 constructs on size exclusion chromatography (SEC)**

(A) Solid line represents polymerized syntaxin binding domain (SBD) in solution; dashed line represents monomeric SBD in reduced solution. (B) Two oligomeric states of Munc13 homology domain (MHD), the former (peak 1) is polymerized, the latter (peak 2) is dimeric. (C) Anion exchange chromatography of M676. (D) M676 shows monomer state in size exclusion chromatography (SEC) buffer. Abs, absorption

**Table 1 Parameters of Munc13-1 constructs determined by analytical ultracentrifugation**

Protein	$M_{CAL}^\dagger$ (kDa)	Sedimentation velocity				$M_{SV}^\ddagger$ (kDa)	Association state
		$S^\ddagger$ (S)	$s_{20,w}^\ddagger$	$ff_0^\S$	$a/b^\S$		
MHD <sup>†</sup>	47.91	3.98	4.10	1.85	12.85	96.32	Dimer
M676	76.88	2.47	2.43	2.13	18.94	65.77	Monomer

<sup>†</sup>  $M_{CAL}$  indicates calculated molecular mass.  $M_{SV}$  indicates molecular mass determined by sedimentation velocity, that is, the ordinate maximum of each peak in the best fit  $c(M)$  distribution. <sup>‡</sup> Apparent sedimentation coefficient  $S$ , the ordinate maximum of each peak in the best fit  $c(s)$  distribution (Fig. 4). The values of apparent sedimentation coefficients  $S$  were corrected to  $s_{20,w}$  for solvent viscosity using the SEDNTERP program, as detailed in "Materials and Methods". <sup>§</sup> The frictional coefficients ( $ff_0$ ) and axial ratios ( $a/b$ ) were calculated using the  $V_{bar}$  method in SEDNTERP. <sup>†</sup> Peak 2 of MHD on size exclusion chromatography.

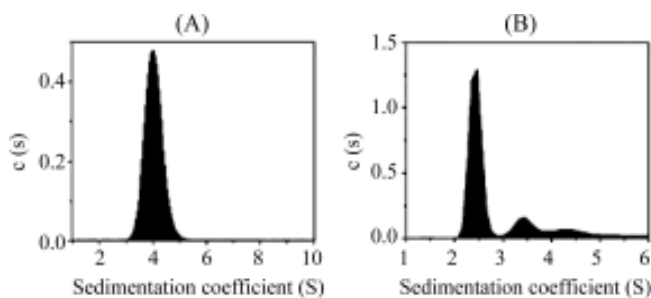


**Fig. 4 Sedimentation coefficient distributions derived from sedimentation velocity profiles of Munc13 homology domain (MHD) (A) and minimal activity domain I (M676) (B)**

(A) Dimeric state of MHD (peak 2 on size exclusion chromatography). (B) Monomeric state of M676. Differential sedimentation coefficients [ $c(s)$ ] were calculated by least square boundary modeling of the sedimentation velocity data using the computer program SEDFIT [19].

a monodispersed population at a dimeric state and were in agreement with the size exclusion gel filtration analysis.

Purified M676 had a sedimenting boundary at 65.77 kDa

with an apparent sedimentation coefficient of 2.47 S [Fig. 4(B) and Table 1], which was consistent with a monodispersed population at the monomeric state of a

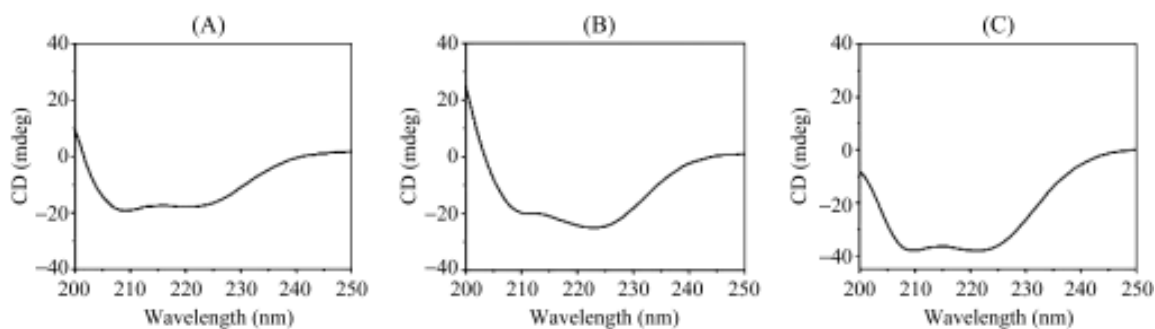


**Fig. 5** Circular dichroism spectrum of Munc13-1 constructs

(A) Reduced syntaxin binding domain (SBD) with 1 mM dithiothreitol. (B) Dimeric Munc13 homology domain (MHD) (peak 2 on size exclusion chromatography). (C) Monomeric minimal activity domain I (M676).

calculated molecular weight of 76.88 kDa.

Based on these data, we concluded that MHD and M676 had distinct properties of monodispersity on particle size and oligomeric state. Furthermore, friction analysis suggested that proteins in both samples assumed an elongated shape (**Table 1**).

#### CD analysis on SBD, MHD and M676

To estimate the secondary structure contents of the purified recombinant proteins of SBD, MHD and M674, the protein samples were subjected to CD analysis using the far ultraviolet spectra in the 190–240 nm range. The CD spectra of all three samples showed characteristic  $\alpha$ -helix features showing a negative band at 210 nm, and a shoulder at approximately 220 nm (**Fig. 5**). Deconvolution of the averaged data points between 200 nm and 240 nm [23] suggested that the SBD recombinant protein had 62%  $\alpha$ -helix, 6%  $\beta$ -strand and 31% random coil contents; the MHD sample had 72%  $\alpha$ -helix, 3%  $\beta$ -strand and 21% random coil contents; and the M676 sample had 65%  $\alpha$ -helix, 5%  $\beta$ -strand and 20% random coil contents. We also analyzed the amino acid sequences of these constructs using the secondary structure prediction algorithm at the Pôle Bioinformatique Lyonnais website (<http://pbil.univ-lyon1.fr/>), which provided a consensus secondary structure based on the results of nine different secondary structure prediction algorithms. Thus, we conclude that all three Munc13-1 recombinant proteins contain significant percentages of  $\alpha$ -helix structural elements.

## Discussion

To study the structures of Munc13 proteins, we used a

mammalian expression system for full-length Munc13-1 [24]. After transient transfection of suspension-growing human 293-EBNA1 cells, an expression vector pTT3 that was cloned with full-length rat Munc13-1 produced low yield undetectable by SDS-PAGE and Coomassie Blue stain (data not shown). Therefore, we focused on the *E. coli* expression system and explored two commercial expression vectors, pET28a and pGEX6p-1. Considering the difficulty that Munc13-1 is a 200 kDa protein that cannot be easily expressed in full length, we designed several functional Munc13-1 fragments, successfully over-expressed them, and purified them with the standard *E. coli* expression system. All constructs are preferred to express at sub-room temperature, 16 °C in particular. Production reaches the maximum in 24 h, and the yield of each construct can be as high as 2 mg per liter of cell culture.

Furthermore, we characterized the monodispersity and stability of the recombinant proteins. Among these constructs, the oligomeric states of MHD [peak 2 in **Fig. 3(B)**] and M676 [**Fig. 3(D)**] were determined, using analytical ultracentrifugation, to be dimeric (96.32 kDa) and monomeric (65.77 kDa), respectively. Both protein samples have desired homogeneities and monodispersities after SEC purification, and maintain their integrity against proteolysis. It is unlikely that the difference between the oligomeric states of MHD and M676 was caused by the non-ionic detergent used to solubilize M676, as the same detergent showed no observable effect on MHD.

Based on the estimation of secondary structure contents (CD analysis) and overall elongated shapes (**Table 1**), we speculate that protein samples assume long helical-bundle like topology, which should be verified by 3-D structure analyses in the future. In addition, the dimeric MHD can be stable for up to 3 d in the presence of 1 mM DTT at 4

°C and, even better, the purified M676 sample maintains good monodispersity and stability as a monomer for at least 1 week. Improved monodispersity and stability of a protein preparation often link to better chances for crystallization, therefore non-ionic detergent Triton X-100 that enhances M676 stability and homogeneity provides ample possibilities for the crystallization trials as well as other *in vitro* functional studies on M676.

Based on the fact that M676 has the minimal activity of Munc13-1 [15] and in light of our new *in vitro* data of the protein properties, we speculate that, unlike M676, MHD could not fold properly. This would suggest that the extra peptide at the N-terminal region in M676 might stabilize the MHD domain, thus enabling an efficient interaction with syntaxin 1A in a cellular environment *in vivo*. In addition, by comparing the protein properties of M676 and M636 *in vitro*, we found that M676 is well behaved, whereas M636 precipitates acutely, suggesting that M676, rather than M636, would be the correct minimal activity domain. Furthermore, considering the poor property of purified SBD, it seems that this unidentified minimal SBD is not sufficient to bind syntaxin 1A *in vitro*. Last, but not least, it is likely that Munc13-1 executes its *in vivo* functions in a monomeric form, as M676 does *in vitro*.

## Acknowledgements

The authors thank Dr. Cai ZHANG for discussions and Dr. Nils BROSE for providing the rat Munc13-1-EGFP vector.

## References

- Klenchin VA, Martin TF. Priming in exocytosis: Attaining fusion-competence after vesicle docking. *Biochimie* 2000, 82: 399–407
- Brenner S. The genetics of *Caenorhabditis elegans*. *Genetics* 1974, 77: 71–94
- Brose N, Rosenmund C, Rettig J. Regulation of transmitter release by Unc-13 and its homologues. *Curr Opin Neurobiol* 2000, 10: 303–311
- Brose N, Hofmann K, Hata Y, Sudhof TC. Mammalian homologues of *Caenorhabditis elegans unc-13* gene define novel family of C<sub>2</sub>-domain proteins. *J Biol Chem* 1995, 270: 25273–25280
- Betz A, Ashery U, Rickmann M, Augustin I, Neher E, Sudhof TC, Rettig J *et al.* Munc13-1 is a presynaptic phorbol ester receptor that enhances neurotransmitter release. *Neuron* 1998, 21: 123–136
- Augustin I, Betz A, Herrmann C, Jo T, Brose N. Differential expression of two novel Munc13 proteins in rat brain. *Biochem J* 1999, 337: 363–371
- Koch H, Hofmann K, Brose N. Definition of Munc13-homology-domains and characterization of a novel ubiquitously expressed Munc13 isoform. *Biochem J* 2000, 349: 247–253
- Rhee JS, Betz A, Pyott S, Reim K, Varoqueaux F, Augustin I, Hesse D *et al.*  $\beta$  phorbol ester- and diacylglycerol-induced augmentation of transmitter release is mediated by Munc13s and not by PKCs. *Cell* 2002, 108: 121–133
- Junge HJ, Rhee JS, Jahn O, Varoqueaux F, Spiess J, Waxham MN, Rosenmund C *et al.* Calmodulin and Munc13 form a Ca<sup>2+</sup> sensor/effector complex that controls short-term synaptic plasticity. *Cell* 2004, 118: 389–401
- Tokumaru H, Augustine GJ. UNC-13 and neurotransmitter release. *Nat Neurosci* 1999, 2: 929–930
- Martin TF. Prime movers of synaptic vesicle exocytosis. *Neuron* 2002, 34: 9–12
- Augustin I, Rosenmund C, Sudhof TC, Brose N. Munc13-1 is essential for fusion competence of glutamatergic synaptic vesicles. *Nature* 1999, 400: 457–461
- Varoqueaux F, Sigler A, Rhee JS, Brose N, Enk C, Reim K, Rosenmund C. Total arrest of spontaneous and evoked synaptic transmission but normal synaptogenesis in the absence of Munc13-mediated vesicle priming. *Proc Natl Acad Sci USA* 2002, 99: 9037–9042
- Betz A, Okamoto M, Benseler F, Brose N. Direct interaction of the rat *unc-13* homologue Munc13-1 with the N terminus of syntaxin. *J Biol Chem* 1997, 272: 2520–2526
- Basu J, Shen N, Dulubova I, Lu J, Guan R, Guryev O, Grishin NV *et al.* A minimal domain responsible for Munc13 activity. *Nat Struct Mol Biol* 2005, 12: 1017–1018
- Stevens DR, Wu ZX, Matti U, Junge HJ, Schirra C, Becherer U, Wojcik SM *et al.* Identification of the minimal protein domain required for priming activity of Munc13-1. *Curr Biol* 2005, 15: 2243–2248
- Lu J, Machius M, Dulubova I, Dai H, Sudhof TC, Tomchick DR, Rizo J. Structural basis for a Munc13-1 homodimer to Munc13-1/RIM heterodimer switch. *PLoS Biol* 2006, 4: E192
- Shen N, Guryev O, Rizo J. Intramolecular occlusion of the diacylglycerol-binding site in the C<sub>1</sub> domain of munc13-1. *Biochemistry* 2005, 44: 1089–1096
- Schuck P. Size-distribution analysis of macromolecules by sedimentation velocity ultracentrifugation and lamm equation modeling. *Biophys J* 2000, 78: 1606–1619
- Whitmore L, Wallace BA. DICHROWEB, an online server for protein secondary structure analyses from circular dichroism spectroscopic data. *Nucleic Acids Res* 2004, 32: W668–W673
- MacGregor EA, Svensson B. A super-secondary structure predicted to be common to several  $\alpha$ -1,4-D-glucan-cleaving enzymes. *Biochem J* 1989, 259: 145–152
- Tsai CJ, Ziegler C. Structure determination of secondary transport proteins by electron crystallography: Two-dimensional crystallization of the betaine uptake system BetP. *J Mol Microbiol Biotechnol* 2005, 10: 197–207
- Andrade MA, Chacon P, Merelo JJ, Moran F. Evaluation of secondary structure of proteins from UV circular dichroism spectra using an unsupervised learning neural network. *Protein Eng* 1993, 6: 383–390
- Durocher Y, Perret S, Kamen A. High-level and high-throughput recombinant protein production by transient transfection of suspension-growing human 293-EBNA1 cells. *Nucleic Acids Res* 2002, 30: E9

Edited by  
Minghua XU